【网络优先出版,实际出版页码及内容以正式版为准】

第55卷第7期 光 子 学 报 Vol.55 No.7
2026年7月 ACTA PHOTONICA SINICA July 2026

引用格式: ZHOU Jiaxin, XIONG Yongkang, WU Minghong, et al. Quality Factor Prediction for Free-Space Optical Communication under Complex Dynamic Environments[J]. Acta Photonica Sinica, 2026, 55(7):0706001
周佳欣,熊永康,吴铭鸿,等.复杂动态环境下的自由空间光通信品质因子预测研究[J].光子学报,2026,55(7):0706001

复杂动态环境下的自由空间光通信品质因子预测研究

周佳欣,熊永康,吴铭鸿,瞿韶明,韩一石*

(广东工业大学 信息工程学院,广州 510006)

摘 要:自由空间光通信(Free Space Optical, FSO)链路在动态大气湍流与天气衰减的共同作用下呈现复杂非线性特性,导致现有算法在链路质量评估中存在拟合能力不足、预测精度低、收敛速度慢及易陷入局部最优的问题。针对这一问题,本文提出一种结合牛顿拉夫逊优化算法(Newton-Raphson-Based Optimizer, NRBO)与反向传播神经网络(Backpropagation Neural Network, BPNN)的链路质量预测算法(NRBO-BPNN),用于预测链路的关键性能指标品质因子,其中NRBO算法通过二阶优化机制迭代更新网络权重,提升BPNN对多维链路参数的非线性拟合与泛化能力。实验结果显示,NRBO-BPNN算法的决定系数达0.985,相比传统BPNN和随机森林算法,其平均绝对误差分别降低69.43%和24.89%,均方根误差降低69.1%和53.35%,这些指标表明该算法在复杂动态环境下具有较高的品质因子预测能力;此外,在150次迭代后,NRBO优化算法的适应度值较遗传算法和粒子群算法分别降低29.86%和14.13%,反映出算法在训练过程中的收敛性能明显提升,为链路性能评估提供可靠依据。

关键词:自由空间光通信;复杂动态环境;品质因子;牛顿拉夫逊优化;反向传播神经网络

中图分类号:TN929.1 **文献标识码**:A **doi**:10.3788/gzxb20265507.0706001

0 引言

近年来,自由空间光(Free Space Optical, FSO)通信凭借高带宽、低时延和强抗电磁干扰等优势,在城市楼宇互联、地面移动组网及应急通信等场景中受到广泛关注[1-2]。然而,受近地大气信道影响,FSO链路传输性能易受湍流及雨雾、沙尘等悬浮颗粒的吸收与散射作用影响,呈现出显著的时变衰减特性,进而影响链路的可靠性[3-4]。为应对这些环境因素导致的链路性能波动,FSO系统通常依赖链路质量状态进行自适应调节[5]。在物理层,通过波束指向的动态调整、湍流抑制、调制优化以及引入混合FSO/射频链路等方法提升链路鲁棒性[6-8];在网络层,通过速率自适应、冗余路由、拓扑重构以及飞行平台部署优化等技术增强复杂动态环境下的网络可用性[9-10]。而上述自适应策略的实施依赖于准确的链路质量状态信息,因此,开展链路质量预测研究对于优化FSO系统性能具有关键意义。

在FSO链路质量预测研究中,机器学习算法凭借其非线性拟合能力得到广泛应用。ALGEDIR A A等以大气衰减情况为特征输入,对多种模型在品质因子预测性能方面进行了对比分析[11]。结果表明,品质因子受环境波动影响呈现显著的非线性特性,线性回归(Linear Regression, LR)与支持向量回归(Support Vector Regression, SVR)的拟合残差较大,而随机森林(Random Forest, RF)表现出更好的鲁棒性。为进一步挖掘更深层信道特征,ESMAIL M A等利用卷积神经网络(Convolutional Neural Network, CNN)实现了对大气湍流影响下的链路光信噪比(Optical Signal-to-Noise Ratio, OSNR)的预测[12]。LIONIS A等将气象

基金项目:国家自然科学基金(No.61471130);广东省重点领域研发计划基金(No.2019B010138004)
第一作者:周佳欣(2001—),女,学生,硕士,主要研究方向为自由空间光通信,链路质量预测方面的研究。Email: Zjoyce629@163.com
通讯作者:韩一石(1970—),男,教授,博士,主要研究方向为自由空间光通信及光纤无线技术等方面的研究。Email: yshan@gdut.edu.cn
收稿日期:2025-12-14;**录用日期**:2026-05-07

参数作为特征输入，开展了对接收信号强度指示的建模研究[13]。该研究引入了结构更为简单的反向传播神经网络（Backpropagation Neural Network, BPNN），且证实了其在捕捉深层非线性映射方面的潜力。SANMUKH K等则针对强湍流环境下的链路环境，利用BPNN实现了对不同大气湍流条件下系统比特错误率（Bit Error Rate, BER）的精确预测[14]。

上述研究验证了机器学习算法在FSO链路预测中的可行性。然而，现有工作仍存在优化空间。首先，部分研究侧重于BER、接收光强等单一指标，其表征能力有限，难以全面反映大气信道对链路质量状态的影响。其次，现有模型往往忽略了大气湍流与天气衰减因素的复合影响，导致其在复杂动态环境下的泛化能力受限。此外，LIONIS A和SANMUKH K等研究所采用的BPNN虽在非线性拟合方面表现良好，但其固有的梯度下降机制在处理高维输入特征时极易陷入局部最优且收敛缓慢。

为此，本文提出了一种结合牛顿拉夫逊优化（Newton-Raphson-Based Optimizer, NRBO）算法与BPNN的品质因子预测算法（NRBO-BPNN）。该模型以品质因子为预测目标，采用Gamma-Gamma分布描述大气湍流效应，结合Beer-Lambert定律刻画天气衰减，以综合反映复杂大气信道对链路性能的影响。而先前研究已表明，这两种模型能够较好地再现真实FSO链路中的主要扰动特性，被广泛用于性能评估和算法验证[15-16]。针对传统梯度下降机制存在的寻优瓶颈，NRBO优化算法通过牛顿-拉夫逊搜索规则（Newton-Raphson Search Rule, NRSR）自适应调整搜索方向，并结合陷阱规避算子（Trap-Avoidance Operator, TAO）增强全局搜索能力，从而有效缓解BPNN在复杂动态环境下的局部最优和收敛缓慢等问题，实现对FSO链路品质因子的强拟合与高精度预测。

1　FSO链路品质因子预测算法设计

1.1　FSO系统链路

FSO系统原理框图如图1所示。在发射端，二进制数据经由马赫-曾德尔调制器（Mach-Zehnder Modulator, MZM）调制到光载波上，形成发射信号。该信号经由大气信道传输时受到衰减与湍流等效应的综合影响，在接收端由光电探测器转换得到的电信号可表示为

$$y=\eta hx+n \tag{1}$$

式中，η为光电探测器响应度；h为传输信道的信道衰落系数；n为加性白高斯噪声。

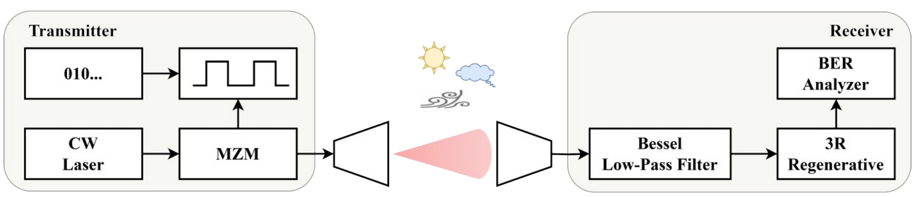

图1　FSO系统原理框图

Fig. 1　Schematic block diagram of FSO system

在FSO链路中，大气信道衰落系数h主要由大气湍流与大气衰减决定，可以表示为[17]

$$h=h_a h_l \tag{2}$$

式中，h_a表示由大气湍流引起的信道衰落，h_l表示不同天气状态下的大气衰减损耗。

Gamma-Gamma分布能较好拟合实验测得的大气湍流效应，可用于描述弱、中、强湍流下的光强波动特性，其概率密度函数表示为[18]

$$f_{h_a}(h_a)=\frac{2(\alpha\beta)^{\frac{\alpha+\beta}{2}}}{\Gamma(\alpha)\Gamma(\beta)}h_a^{\frac{\alpha+\beta}{2}-1}K_{\alpha-\beta}\left(2\sqrt{\alpha\beta h_a}\right) \tag{3}$$

式中，$\Gamma(\cdot)$表示Gamma函数；$K_{\alpha-\beta}(\cdot)$为第二类$\alpha-\beta$阶修正贝塞尔函数，α和β分别对应大尺度与小尺度湍流参数，其计算公式分别为

$$\alpha=\left(\exp\left(\frac{0.49\sigma_R^2}{\left(1+1.11\sigma_R^{12/5}\right)^{7/6}}\right)-1\right)^{-1} \tag{4}$$

$$\beta=\left(\exp\left(\frac{0.51\sigma_R^2}{\left(1+0.69\sigma_R^{12/5}\right)^{5/6}}\right)-1\right)^{-1} \tag{5}$$

式中，$\sigma_R^2=1.23C_n^2k^{7/6}L^{11/6}$为Rytov方差；$k=2\pi/\lambda$为空间波数，$\lambda$为波长，$L$为传输距离；$C_n^2$为大气折射率结构常数，其决定了湍流的强度，在本文中弱湍流下取$C_n^2=10^{-16}$，中湍流下取$C_n^2=10^{-15}$，强湍流下取$C_n^2=10^{-14}$[19]。

大气衰减随时间动态变化，其物理机制可由Beer-Lambert定律定量描述，计算公式为[20]

$$h_l=e^{-a_lL} \tag{6}$$

式中，L表示链路长度，a_l表示与波长及天气状态相关的衰减系数，其通过Kim模型与能见度V以及波长λ关联

$$a_l=\frac{3.91}{V}\left(\frac{\lambda}{550}\right)^{-q} \tag{7}$$

式中，q为反映大气中颗粒的尺度及浓度分布特性的修正因子，可表示为

$$q(V)=\begin{cases}1.6, & V>50\text{km}\\ 1.3, & 6<V<50\text{km}\\ 0.16V+0.34, & 1<V<6\text{km}\\ V-0.5, & 0.5<V<1\text{km}\\ 0, & V<0.5\text{km}\end{cases} \tag{8}$$

能见度V的取值范围根据不同天气状态确定，如表1所示[21]。修正因子$q(V)$则根据每个样本对应的V值实时匹配公式(8)中的分段计算规则。

接收端通过光电探测器进行光电转换，随后经滤波、采样与判决过程恢复原始数据，并基于眼图分析计算品质因子以评估链路性能。在FSO链路性能评估中，品质因子Q定义为信号电压均值μ与噪声标准差σ之比，可表示为

$$Q=\frac{\left|\mu_1-\mu_0\right|}{\sigma_1+\sigma_0} \tag{9}$$

而与系统BER存在如下确定关系[22]

$$BER=\frac{1}{2}\operatorname{erfc}\left(\frac{Q}{\sqrt{2}}\right)\approx\frac{\exp\left(-Q^2/2\right)}{Q\pi} \tag{10}$$

表1 基于能见度范围的天气状况分类

Table 1 Classification of weather conditions based on visibility range

Parameters	Value(km)
Clear	>20
Haze	2.8 - 20
Rain	1−2.8
Fog	<1

1.2 预测算法数据集构建

本文以采用OOK调制的FSO链路为研究对象，通过数值仿真方式生成算法数据集。大气信道模块综合考虑湍流效应与大气衰减的叠加影响，其中湍流效应采用Gamma-Gamma分布模型描述，天气衰减基于Beer-Lambert定律计算，仿真中采用分层均匀采样策略生成3850组样本。具体的数据集分布情况为：首先，依据天气状态（晴、霾、雨、雾）进行数据集的等比例均分，接着在每种天气状态内部，针对不同的大气湍流强度（弱、中、强）再次执行等比例划分，确保各类天气状态和湍流强度数据分布均匀。在上述构成的多维物理

子层内，对发射功率、链路距离及光束发散角等连续参数在其取值范围内进行独立随机采样，采样步长精细至0.1，从而有效避免了因采用单一数值导致的算法泛化能力不足。

在眼图仿真与特征提取阶段，通过每比特64点采样离散化接收端电信号，并综合考虑探测器背景热噪声与受瞬时光强调制的散粒噪声。同时，所有样本在提取品质因子前均经功率归一化与低通滤波，以消除功率基准差异对信道特征提取的影响。系统仿真主要参数及其取值范围见表2。

表2 OOK-FSO仿真系统设计参数

Table 2 OOK-FSO simulation system design parameters

Parameters	Value	Parameters	Value
Wavelength/nm	1550	Transmitter power /mW	5—25
Bit rate /Gbps	10	Transmitter aperture /cm	10
Samples per bit	64	Beam divergence angle /mrad	2—5
$C_n^2/\mathrm{m}^{-2/3}$	10^{-16}、10^{-15}、10^{-14}	Visibility/km	0.5—25
Link distance /km	0.1—5	Receiver aperture /cm	20

1.3 基于NRBO-BPNN的品质因子预测算法

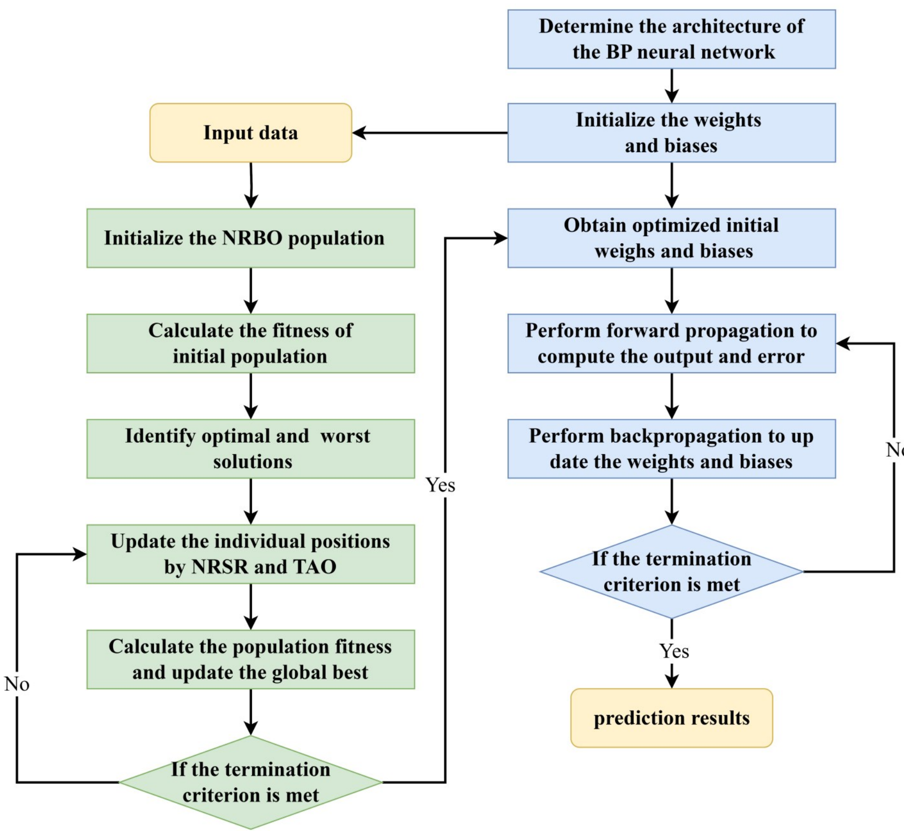

图2 NRBO-BPNN算法流程图

Fig. 2 Flowchart of the NRBO-BPNN algorithm

基于NRBO-BPNN的FSO链路品质因子预测算法的训练流程如图2所示，主要流程如下：

种群初始化：以随机方式生成初始解集合，每个解代表一组待优化的BPNN初始权重和偏置。该初始化策略有助于维持种群多样性，避免算法早熟收敛。初始化位置计算公式为

$$x_j^n = lb \times rand(ub - lb), n = 1, 2, \ldots, N_p 且 j = 1, 2, \ldots dim \tag{11}$$

式中，x_j^n表示第n个解在第j维上的取值，lb和ub分别为搜索空间的下界和上界，$rand$为取值在[0, 1]范围内的随机数，N_p为种群规模，dim为解的维数。

NRSR搜索机制：通过利用目标函数的梯度与Hessian矩阵推算解的更新位置，以提高迭代精度与收敛

速度。在每次迭代中，梯度和Hessian矩阵共同决定更新方向和步长，更新步长表示为

$$\triangle x = -\frac{f'(x)}{f''(x)} \tag{12}$$

式中，$f'(x)$为目标函数在当前解x处的一阶导数（梯度），反映误差随权重变化的趋势；$f''(x)$为目标函数在当前解x处的二阶导数（Hessian矩阵），反映误差曲面的曲率信息。其中，目标函数为BPNN在训练集上的均方误差。该更新规则通过目标函数的二阶泰勒展开推导得出，旨在利用梯度与曲率信息引导解向局部最优方向更快收敛。当二阶导数无法计算时，算法引入变异机制维持有效搜索。

陷阱规避算子TAO：每次迭代生成一个服从均匀分布的随机数$r \in [0,1]$，当$r < DF$时激活TAO机制，其中DF为激活概率。激活后，算法根据随机生成的两组权重参数$\mu_1, \mu_2 \in [0,1]$和两组扰动因子$\theta_1 \in [-1,1]$，$\theta_2 \in [-0.5, 0.5]$来生成两种更新方式。若$\mu_1 < 0.5$，则依据当前解与最优解的差异乘以θ_1施加扰动，使解向最优解附近探索；否则以种群均值加上θ_2的随机偏移引导解分布，使解向群体聚集区域靠拢。μ_2用于调节两种更新方式下的扰动幅度，与扰动因子共同控制解的更新步长。扰动整体强度由自适应系数δ控制，该系数随迭代次数非线性衰减，使算法初期探索性强，后期逐步收敛至优质区域。通过上述机制，TAO能够有效防止算法过早陷入局部最优，提升全局寻优能力。

BPNN训练：经NRBO优化后，得到最优初始权值和偏置，并将其用于BPNN的参数初始化。网络由输入层、隐藏层与输出层构成，神经元之间通过权值矩阵全连接形成非线性映射。前向传播阶段，隐藏层单元的输出表示为

$$y_j = f\left(\sum_{i=1}^{n} \boldsymbol{W}_{ji} x_i + b_j\right) \tag{13}$$

式中，y_j为输出值，x_i为输入值，$\boldsymbol{W}_{ji}$为权重矩阵，b_j为偏置，f为激活函数。

2　仿真结果与讨论

2.1　评估指标及算法参数

为系统评估预测算法的综合性能，本文选取三项指标进行量化评价：决定系数（Coefficient of Determination, R^2）、平均绝对误差（Mean Absolute Error, MAE）和均方根误差（Root Mean Squared Error, RMSE）。R^2衡量预测值与真实值的拟合程度，值越接近1表示算法拟合越好；MAE反映整体误差水平，值越低表示预测精度越高；RMSE对异常偏差敏感，值越低表示算法预测稳定性越好。具体计算公式可分别表示为

$$R^2 = 1 - \frac{\sum_{i=1}^{n}(y_i - \hat{y}_i)^2}{\sum_{i=1}^{n}(y_i - \bar{y})^2} \tag{14}$$

$$MAE = \frac{1}{n}\sum_{i=1}^{n}\left|y_i - \hat{y}_i\right| \tag{15}$$

$$RMSE = \sqrt{\frac{1}{n}\sum_{i=1}^{n}(y_i - \hat{y}_i)^2} \tag{16}$$

在参数设置方面，首先通过预实验对学习率、种群规模及最大迭代次数等超参数进行系统性寻优，确定的基础训练配置如表3所示。

隐藏层神经元数量l作为决定模型拓扑结构与非线性映射能力的核心参数，其取值直接决定了网络的

表3　NRBO-BPNN实验参数设置

Table 3　Experimental parameter settings of the NRBO-BPNN algorithm

Parameters	Value	Parameters	Value
Neurons in the input layer	5	Maximum iterations	1000
Learning rate	1×10^{-3}	Population size	20
Convergence threshold	10^{-6}	Decision factor for TAO	0.6

表征上限。为此，本文参考经验公式 $l=\sqrt{N+K}+\varepsilon$ 初步确定取值范围，其中 N 和 K 分别代表输入和输出神经元数目，ε 为[1, 10]之间的常数[23]；此外，隐藏层神经元数量应介于输入层与输出层大小之间，通常可取输入层大小的2/3加上输出层大小[24]。综合上述原则，本文将搜索空间设为[3, 10]，并进行参数敏感性分析，具体结果见表4。

表4 不同隐藏层神经元数量下的性能指标对比

Table 4 Comparison of prediction performance under different numbers of hidden layer neurons

	R2	MAE	RMSE
3	0.942	9.842	16.524
4	0.971	6.852	11.237
5	**0.985**	**5.390**	**9.708**
6	0.981	6.427	11.458
8	0.973	7.961	13.883
10	0.962	9.449	16.126

可以看出，随着节点数增加，算法对非线性特征的表征能力呈现先增强后衰减的规律。当神经元数量为5时，测试集的 R^2 达到峰值0.985，且MAE与RMSE均取得极小值。随神经元数量的增加，测试集性能呈现过拟合特征。综合权衡预测精度与计算开销，本文将隐藏层神经元数最终设定为5。

2.2 不同算法预测性能对比

为准确预测复杂动态环境下FSO链路的品质因子，本文对比了多种机器学习算法在该场景下的预测能力，并与所提出的NRBO-BPNN算法进行了性能比较。在此基础上，进一步分析了NRBO-BPNN算法在不同天气状况与大气湍流下的独立预测表现。

从表5中可看出NRBO-BPNN算法在 R^2、MAE和RMSE三项指标上均优于对比算法，展现出更高的预测精度和稳定性。LR与SVR算法的预测性能表现较差，R^2 分别仅为0.437和0.715，不适用于复杂动态环境下FSO链路品质因子的高精度预测。长短期记忆网络(Long Short-Term Memory, LSTM)作为处理时序数据的经典算法，在动态环境数据中具有一定优势。然而，LSTM的复杂门控结构导致其参数量较大，在处理复杂的非线性关系时，LSTM的 R^2 低于BPNN、RF、CNN和NRBO-BPNN等非递归算法。而其中，NRBO-BPNN算法的 R^2 达到0.985，显示出优异的拟合与解释能力。在误差指标方面，NRBO-BPNN算法同样表现出色，其MAE较CNN、BPNN和RF分别降低68.17%、69.43%和24.89%，RMSE分别下降65.54%、69.1%和53.35%。以上结果证明，所提出的NRBO-BPNN算法中具备更优的预测精度、泛化能力和稳定性，适用于复杂动态环境下FSO链路中品质因子的可靠预测。

表5 复杂动态环境下不同预测算法评价指标对比

Table 5 Comparison of evaluation metrics of different prediction algorithms under complex dynamic conditions

算法	R2	MAE	RMSE
LR	0.437	56.888	104.052
SVR	0.715	69.308	74.045
LSTM	0.942	18.521	29.142
CNN	0.959	16.935	28.172
BPNN	0.949	17.631	31.414
RF	0.977	7.176	20.811
NRBO－BPNN	**0.985**	**5.390**	**9.708**

图3进一步展示了仿真测试集中部分样本的品质因子真实值与NRBO-BPNN模型预测值的对比。此外，由于两者量纲相同，为便于观察拟合趋势，两者均进行了归一化处理。可以看到，NRBO-BPNN算法的预测值(蓝色线)与实际值(红色点)高度吻合，表明该算法能够有效拟合样本中的变化趋势。尽管存在一些小的波动，整体预测值准确地跟踪了实际数据的波动，体现了NRBO-BPNN算法在该任务中的高预测精度和稳定性。

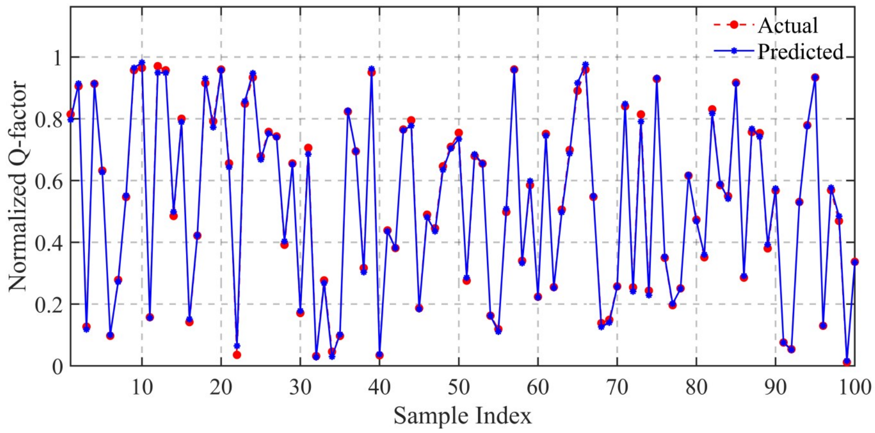

图3 仿真归一化品质因子与NRBO-BPNN预测值对比

Fig. 3 Comparison of simulated and NRBO-BPNN predicted normalized Q-factors

图4展示了CNN、BPNN、RF与NRBO-BPNN算法在晴天、霾天、雨天和雾天四类天气状态下的品质因子预测性能。图4(a)展示了各算法在不同天气状态下的R^2对比。CNN、BPNN在雾天受能见度影响,R^2急剧下降至0.770附近,RF下降至0.837;而NRBO-BPNN算法在所有天气状态下均取得最高R^2值,雾天下R^2仍可达0.974,表明其预测结果与真实值之间具有最佳拟合优度。图4(b)表明,NRBO-BPNN在四类天气下均保持最低MAE。在霾天条件下,其MAE为5.729,相较CNN、BPNN和RF分别降低约68.07%、71.04%和26.25%;在雨天进一步降至4.733,较RF下降约16.59%;雾天的MAE仅为2.887,体现了其预测偏差最小的优势;晴天的MAE为9.142略高于其他天气,这是由于晴天品质因子本身波动幅度较小,单个预测偏差在绝对误差上占比相对突出,但NRBO-BPNN仍保持各算法中最优的预测性能。图4(c)显示,NRBO-BPNN在RMSE指标上同样保持最优。在霾天,其RMSE为8.753,相较CNN、BPNN和RF分别降低约67.84%、74.72%和56.68%;在雨天为9.197,较RF下降约45.25%。即便在能见度最差的雾天,其RMSE仍为8.726,相较三者分别降低66.04%、65.54%和59.76%,体现出更强的稳定性和抗波动能力,说明其预测稳定性最高,对异常值不敏感。综合来看,NRBO-BPNN算法在所有评价指标和天气状态下均表现出显著的优越性,验证了其强拟合与高精度性。

如图5所示,不同算法在弱、中、强湍流下的性能差异明显。图5(a)展示了各算法在不同湍流强度下的R^2对比。值得注意的是,CNN与BPNN的性能在中湍流下即开始显著下滑,至强湍流时,R^2分别降至0.905和0.943;相比之下,RF在强湍流下的R^2仍能保持约0.967,但NRBO-BPNN表现最为优异且稳定,在强湍流下的R^2高达0.988。图5(b)展示了各算法在MAE指标上的表现。CNN的MAE呈现随湍流增强而逐渐下降的趋势,但最低仍达14.214;BPNN的MAE在弱湍流为16.642,在中度湍流显著升高至20.989,而在强湍流下降至15.025,呈现中湍流峰值特征,表明其对湍流扰动敏感且存在非线性响应;RF的MAE在弱、中、强湍流下分别为9.706、6.648和7.074,表现出较高稳定性;而NRBO-BPNN整体数值远低于其他算法,说明其预测偏差受湍流影响最弱。从图5(c)的RMSE结果来看,CNN的RMSE随着湍流强度的增强呈逐渐下降趋势,但在强湍流下仍达24.151;BPNN算法在中、强湍流下的RMSE分别为35.701和32.896,中湍流达到峰值; RF算法在弱、中、强湍流下的RMSE分别为25.371、17.268和18.443,相较于其他算法表现出相对稳定的变化趋势;而NRBO-BPNN算法在弱、中、强湍流下的RMSE分别为12.476、9.739和4.745,整体数值最低且呈平滑下降趋势,进一步验证了其优化训练策略与参数更新机制能够有效抑制湍流扰动,保持较高的预测精度。

2.3 不同优化算法比较

图6对比了遗传算法(Genetic Algorithm, GA)、粒子群优化算法(Particle Swarm Optimization, PSO)与NRBO在BPNN参数优化中的性能。GA初始适应度约0.0151,迭代至约20次后快速下降至0.0107附近,并进入停滞状态;PSO的初始适应度为0.0172,虽在迭代过程中可下降至0.0087,但仍存在持续振荡,表明其探索阶段与开发机制协调不足;相比之下,NRBO初始适应度约0.0086,迭代过程中平稳下降,并最终收

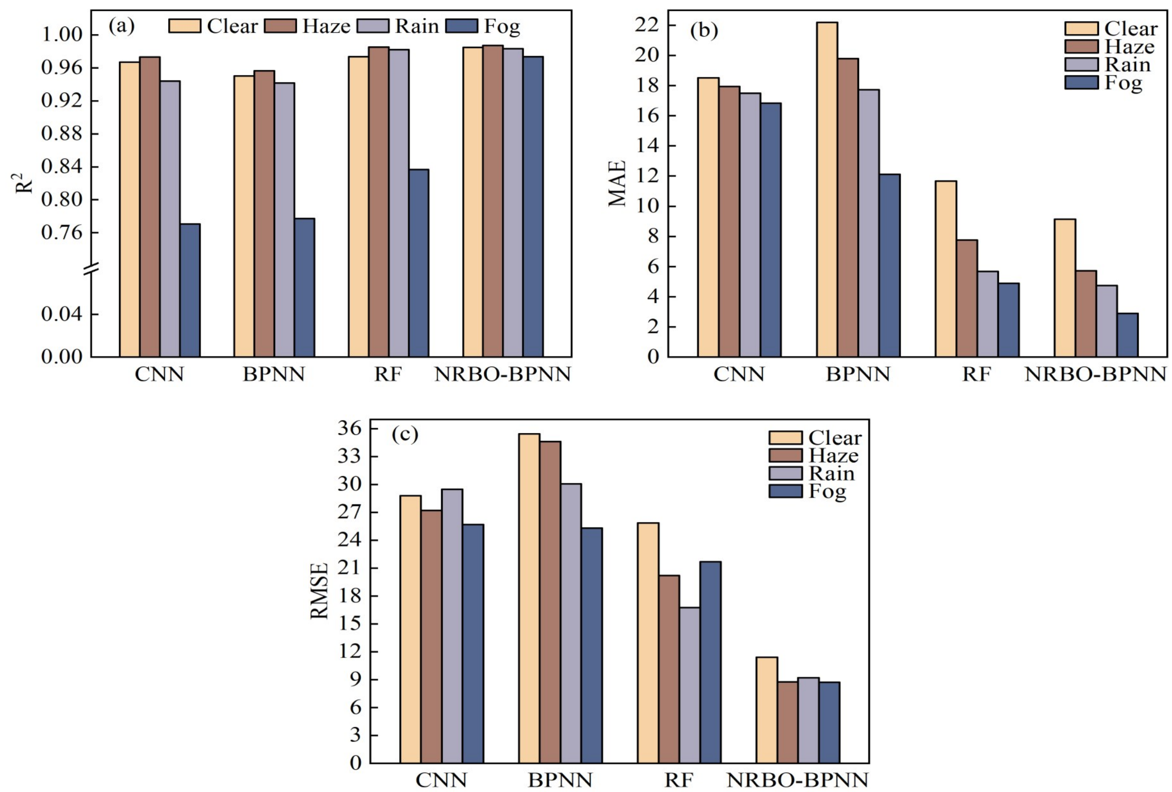

图4　不同天气状态下的预测算法评价指标对比。(a) R^2; (b) MAE; (c) RMSE

Fig. 4　Comparison of prediction algorithm evaluation metrics under different weather conditions. (a) R^2; (b) MAE; (c) RMSE

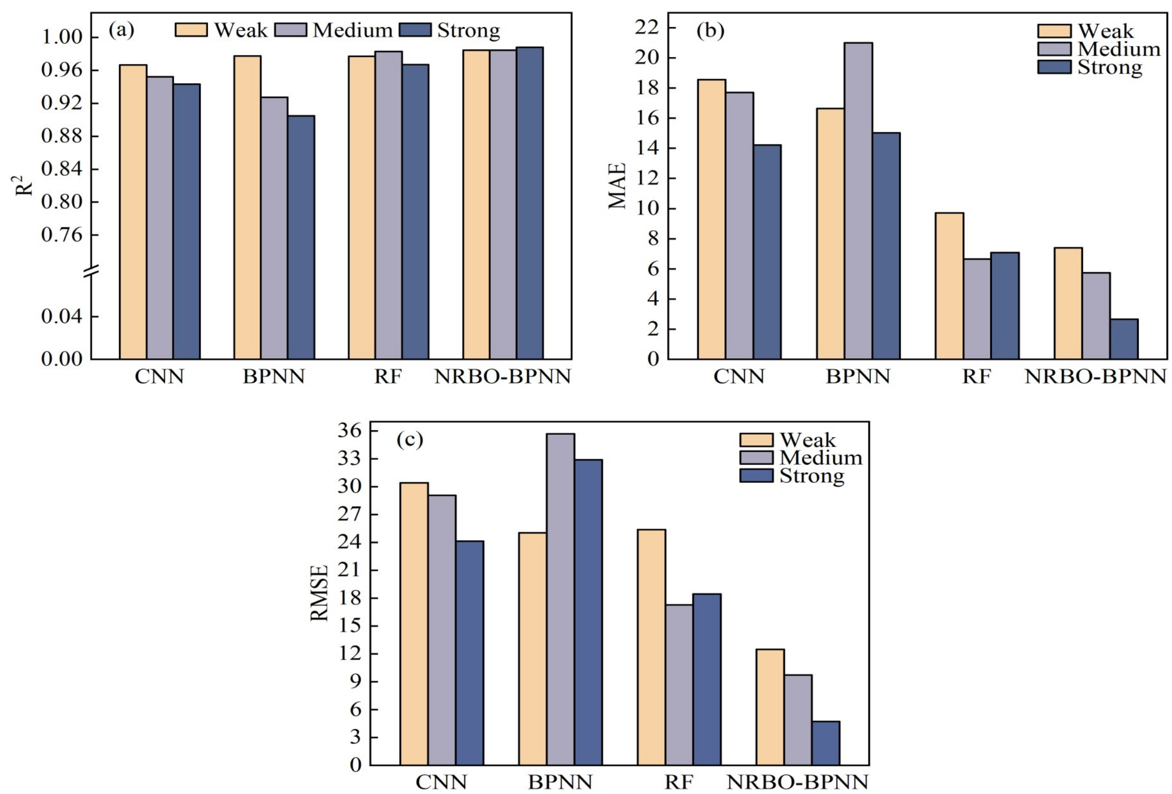

图5　不同大气湍流强度下的预测算法评价指标对比。(a) R^2; (b) MAE; (c) RMSE

Fig. 5　Comparison of prediction performance metrics under different atmospheric turbulence intensities. (a) R^2; (b) MAE; (c) RMSE

敛至更低水平。实验数据表明,NRBO算法在收敛后适应度值较GA降低了29.86%,较PSO降低了14.13%,且自收敛后至第150次始终保持稳定无波动,充分验证了其在寻优精度和稳定性上的显著优势。

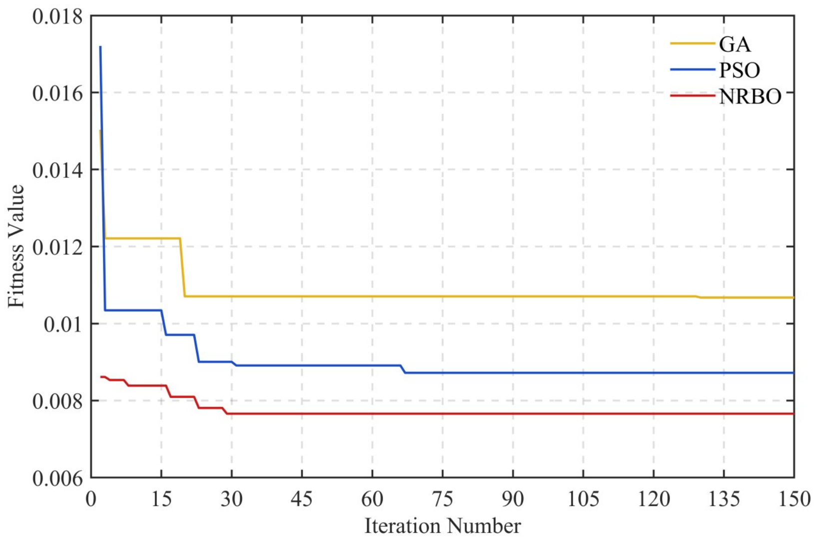

图6 不同优化算法下BPNN的适应度收敛曲线

Fig. 6 Fitness convergence curves of BPNN under different optimization algorithms

表6从R^2、MAE和RMSE三项评价指标评估了GA-BPNN、PSO-BPNN和NRBO-BPNN三个算法预测品质因子的性能。结果表明,NRBO-BPNN算法在所有评价指标上均展现出显著优势:其R^2值较GA-BPNN和PSO-BPNN分别提升2.99%和3.27%,呈现出更优的拟合能力;对于误差指标,NRBO-BPNN的MAE和RMSE相较于GA-BPNN大幅下降65.5%和57.3%,相较于PSO-BPNN也降低了67.6%和47.0%,验证了其在预测精度方面的显著优势。

表6 三种优化算法对BPNN性能影响的对比

Table 6 Comparison of the effects of three optimization algorithms on BPNN performance

算法	R^2	MAE	RMSE
GA－BPNN	0.956	15.642	29.994
PSO－BPNN	0.954	12.626	18.324
NRBO－BPNN	**0.985**	**5.390**	**9.708**

3 结论

本文针对复杂动态环境下FSO链路品质因子预测中存在的拟合能力不足、预测精度低及收敛性能不足的问题,提出了一种基于NRBO的BPNN预测算法(NRBO-BPNN)。实验结果表明,该算法表现出卓越的拟合能力,在完整测试集上,其决定系数R^2高达0.985,明显优于CNN(0.959)、BPNN(0.949)和RF(0.977)。在误差指标上,NRBO-BPNN的平均绝对误差MAE为5.390,较CNN、BPNN和RF分别降低68.17%、69.43%和24.89%,均方根误差RMSE为9.708,分别降低65.54%、69.1%和53.35%,显示出显著的预测精度。在不同天气状态下,NRBO-BPNN同样保持优异表现。在雾天,其R^2达到0.974,MAE仅为2.887,RMSE为8.726,相较其他算法最大下降幅度超过60%,显示出对能见度下降影响的高度鲁棒性。针对大气湍流强度变化,NRBO-BPNN在弱、中、强湍流下的R^2相较于对比算法达到最高值,RMSE从12.476下降至4.745,证明其预测偏差受扰动影响最小。在参数优化方面,NRBO算法在150次迭代后适应度值较遗传算法降低29.86%,较粒子群算法降低14.13%,收敛速度更快且更稳定。

综上,NRBO-BPNN算法在复杂动态环境下实现了FSO链路品质因子预测的强拟合、高精度和快收敛,充分验证了其优化训练策略和二阶参数更新机制的有效性,为链路性能评估和系统可靠性分析提供了坚实依据。为进一步提升NRBO-BPNN算法的泛化能力与实用性,后续研究将引入仿真建模与实测微调

相结合的迁移学习策略，通过少量实测关键样本对该算法进行参数化校准，使其能精准适配真实链路环境，无需依赖大规模实测数据采集。如何在复杂多变的真实信道中构建有效的关键样本选择机制，将是实现知识迁移的核心难点。因此，本文现阶段优先通过覆盖多类物理特征的完备仿真确立稳健的NRBO-BPNN算法基准，为后续在真实环境中执行高效校准与知识迁移奠定基础。

参考文献

[1] HASSNAIN A S M, ASGHAR M K, HUSSAIN A. Hybrid FSO/RF networks: A review of practical constraints, applications and challenges[J]. Optical Switching and Networking, 2023, 47: 100697.

[2] GAO W, DONG K, JIANG L, et al. Composite channel modeling and experimental investigation of free-space optical communications for urban scenario applications[J]. Optics express,2025,33(20):42370-42384.

[3] CHOW C W. Recent advances and future perspectives in optical wireless communication, free space optical communication and sensing for 6G[J]. Journal of Lightwave Technology, 2024, 42(11): 3972-3980.

[4] ZHAO Xiongwen, ZHANG Yu, QIN Peng, et al. Key Technologies and Development Trends for a Space-Air-Ground Integrated Wireless Optical Communication Network[J]. Acta Electronica Sinica,2022,50(01):1-17.
赵雄文，张钰，秦鹏，等.空天地一体化无线光通信网络关键技术及其发展趋势[J].电子学报，2022,50(01):1-17.

[5] SABER J M, SHOKOUHIFAR M, ANSARI S I. Performance analytics of adaptive subcarrier intensity modulated free-space optical communications over general Málaga turbulence links[J]. Results in Optics, 2024, 14:100614.

[6] TONINI F, RAFFAELLI C, WOSINSKA L, et al. Cost-optimal deployment of a C-RAN with hybrid fiber/FSO fronthaul[J]. Journal of Optical Communications and Networking, 2019, 11(7): 397-408.

[7] QADY E A, ABAZA M. Performance analysis of the effects of atmospheric turbulence on free space optical communication using multi-hop decode and forward relay in north and south of Egypt[J]. Optical and Quantum Electronics, 2024, 56(8): 1373.

[8] YAO H F, WANG W H, ZHOU C, et al. Optical adaptive power control based on atmospheric channel reciprocity for mitigating turbulence disturbances in free-space optics communication[J]. Optics Express, 2023, 31(22): 36992-37010.

[9] KALESNIKAU I, PIÓRO M, RAK J, et al. Enhancing resilience of FSO networks to adverse weather conditions[J]. IEEE Access, 2021, 9: 123541-123565.

[10] GU Z Q, ZHANG J W, JI Y F. Topology optimizing in FSO-based UAVs relay networks for resilience enhancement[J]. Mobile Networks and Applications, 2020, 25(1): 350-362.

[11] ALGEDIR A A, ELGANIMI T Y. Machine Learning Models for Predicting the Quality Factor of FSO Systems with Multiple Transceivers[C]. 2020 2nd Global Power, Energy and Communication Conference (GPECOM), 2020: 308-311.

[12] ESMAIL M A, SAIF W S, RAGHEB A M, et al. Free space optic channel monitoring using machine learning [J]. Optics Express, 2021, 29(7): 10967-10981.

[13] LIONIS A, PEPPAS K, NISTAZAKIS H E, et al. Using machine learning algorithms for accurate received optical power prediction of an FSO link over a maritime environment[J]. Photonics, 2021, 8(6): 212.

[14] SANMUKH K, AANCHAL S. Performance estimation of SISO and MIMO Ro-FSO link under atmospheric turbulence [J]. Optical and Quantum Electronics, 2023, 56(1): 48.

[15] NIU M B, CHENG J L, Holzman J F. Exact error rate analysis of equal gain and selection diversity for coherent free-space optical systems on strong turbulence channels[J]. Optics Express, 2010, 18(13): 13915-13926.

[16] FARID A A. HRANILOVIC S. Outage capacity optimization for free-space optical links with pointing errors[J]. Journal of Lightwave technology, 2007, 25(7): 1702-1710.

[17] MALIK S, SAHU P K. Free space optics/millimeter-wave based vertical and horizontal terrestrial backhaul network for 5G[J]. Optics Communications, 2020, 459: 125010.

[18] BHOWAL A, KSHETRIMAYUM R S. Advanced spatial modulation systems[M]. Singapore: Springer, 2021.

[19] ÁLVAREZ-ROA M, ÁLVAREZ-ROA C, FERNÁNDEZ-ARAGÓN F, et al. Performance analysis of atmospheric optical communication systems with spatial diversity affected by correlated turbulence[J]. Journal of Optical Communications and Networking, 2022, 14(7): 524-539.

[20] DABIRI M T, SADOUGH S M S, KHALIGHI M A. Channel modeling and parameter optimization for hovering UAV-based free-space optical links[J]. IEEE Journal on Selected Areas in Communications, 2018, 36(9): 2104-2113.

[21] GHASSEMLOOY Z, POPOOLA W, RAJBHANDARI S. Optical Wireless Communications: System and Channel Modelling with MATLAB®, Second Edition[M]. Boca Raton: CRC Press, 2019.

[22] BURDAH S, ALAMTAHA R, SAMIJAYANI O N, et al. Performance analysis of Q factor optical communication in free space optics and single mode fiber[J]. Universal Journal of Electrical and Electronic Engineering, 2019, 6(3): 167-175.

[23] HOU S K, LIU Y R, ZHANG K. Prediction of TBM tunnelling parameters based on IPSO-BP hybrid model[J]. Chinese

Journal of Rock Mechanics and Engineering, 2020, 39(08): 1648-1657.
侯少康，刘耀儒，张凯．基于IPSO-BP混合模型的TBM掘进参数预测[J].岩石力学与工程学报，2020，39(08)：1648-1657.

[24] SEIDI E, KAVIARI F, MILLER F S. Hyperparameter Tuning of Artificial Neural Network-Based Machine Learning to Optimize Number of Hidden Layers and Neurons in Metal Forming[J]. Journal of Manufacturing and Materials Processing, 2025, 9(8): 260.

Quality Factor Prediction for Free-Space Optical Communication under Complex Dynamic Environments

ZHOU Jiaxin, XIONG Yongkang, WU Minghong, QU Shaoming, HAN Yishi*

(*School of Information Engineering*, *Guangdong University of Technology*, *Guangzhou*, *Guangdong*, 510006, *China*)

Abstract: Free space optical (FSO) communication systems have emerged as an important complement to conventional fiber-optic and radio-frequency (RF) communication technologies due to their inherent advantages, including ultra-high bandwidth, high data transmission rates, low latency, and operation in license-free spectrum bands. These characteristics make FSO systems particularly attractive for medium- and short-range high-speed wireless transmission scenarios such as satellite communications, unmanned aerial vehicle (UAV) relays, emergency communications, and last-mile access networks. Despite these advantages, the practical deployment and stable operation of FSO systems are significantly challenged by their strong sensitivity to atmospheric conditions. In realistic propagation environments, FSO link performance is highly susceptible to dynamic and complex environmental factors, including atmospheric turbulence, fog, haze, rain, and dust. These effects introduce severe nonlinear distortions and random fluctuations in received optical signals, leading to time-varying attenuation, signal fading, and degradation of link quality. Consequently, transmission stability and reliability are difficult to guarantee, especially under rapidly changing weather conditions. To mitigate performance degradation, numerous adaptive optimization strategies have been proposed, such as adaptive modulation, power control, beam adjustment, and hybrid FSO/RF link switching. However, the effectiveness of these strategies fundamentally relies on the availability of accurate and real-time link quality assessment or prediction. Traditional physical channel models often require simplified assumptions and struggle to capture the highly nonlinear and time-varying characteristics of real-world FSO channels. Although machine learning-based methods have recently been introduced for link quality prediction, existing approaches still face notable limitations, including insufficient nonlinear fitting capability, limited prediction accuracy, slow convergence speed, and vulnerability to local optima. These shortcomings restrict their applicability in complex dynamic environments. Therefore, developing a robust and accurate Q-factor prediction algorithm with enhanced fitting capability, high prediction accuracy, and stable training behavior is of critical importance. This study aims to address these challenges by proposing an improved data-driven prediction framework for FSO link quality under complex dynamic weather conditions. This study proposes a Q-factor prediction algorithm for FSO links employing on - off keying (OOK) modulation, referred to as the Newton-Raphson-Based Optimizer Backpropagation (NRBO-BP) algorithm. The proposed method integrates the Newton-Raphson-based optimizer (NRBO) with a Backpropagation Neural Network (BPNN) to establish an accurate nonlinear mapping between physical link parameters and the corresponding Q-factor, thereby improving both prediction accuracy and training stability. First, multidimensional input features are constructed based on the physical characteristics of the FSO system. These features include transmit power, link distance, beam divergence angle, atmospheric refractive index structure constant, and atmospheric visibility under different weather conditions. Such a feature design ensures comprehensive characterization of both system-level and environmental factors influencing link quality. The output label is defined as the Q-factor calculated using a theoretical OOK-based FSO link model, ensuring data consistency and reliability during training. To overcome the limitations of conventional gradient-based optimization, the NRBO is employed to optimize the neural network parameters. The Newton - Raphson search rule utilizes second-order gradient information to precisely determine the weight update direction, enabling faster and more accurate convergence. Furthermore, when the curvature of the optimization landscape approaches zero or when continuous stagnation occurs along a certain search direction, a trap-avoidance operator is activated. This operator introduces adaptive perturbations that allow the optimization process to escape flat regions and local optima. By suppressing ineffective update paths and enhancing productive exploration, NRBO effectively reduces redundant updates, parameter oscillations, and training instability. After NRBO-based initialization and optimization, the neural network undergoes end-to-end training through standard gradient backpropagation. The optimized initial parameters significantly accelerate error convergence and improve robustness against channel dynamics, ultimately enhancing the predictive capability of the model in complex environments. Simulation results demonstrate that the proposed NRBO-BP algorithm exhibits significant advantages in predicting the Q-factor of FSO links under complex dynamic environmental conditions. Performance evaluation conducted on the complete test dataset shows that NRBO-BP achieves superior results across all evaluation metrics, including the coefficient of determination (R^2), mean absolute error (MAE), and root mean square error (RMSE). Specifically, NRBO-BP achieves an R^2 value of 0.985, indicating an excellent fit between predicted and actual Q-factor values. Compared with convolutional neural networks (CNN), conventional BPNN, and random forest (RF) models, the MAE is reduced by approximately 68.17%, 69.43%, and 24.89%, respectively. Similarly, RMSE is reduced by approximately 65.54%, 69.1%, and 53.35%, respectively. These results confirm the strong adaptability and robustness of the proposed algorithm under varying atmospheric conditions. Further analysis of optimization performance reveals that NRBO provides faster convergence and more stable training compared to genetic algorithm (GA) and particle swarm optimization (PSO). The final convergence fitness of NRBO is approximately 29.86% lower than that of GA and 14.13% lower than that of PSO, demonstrating its superior optimization efficiency. When combined with BP neural networks, NRBO-BP achieves approximately 3% improvement in R^2 compared to GA-BP and PSO-BP, while MAE and RMSE are consistently reduced. These results highlight the effectiveness of NRBO in enhancing convergence behavior and strengthening the predictive capability of neural networks. This paper addresses the challenge of accurately predicting FSO link quality in complex dynamic environments, with a specific focus on Q-factor prediction. Traditional physical models struggle to characterize nonlinear channel behavior, while existing neural network-based approaches often suffer from limited accuracy, slow convergence, and susceptibility to local optima. To overcome these challenges, a BP neural network integrated with a Newton-Raphson-based optimizer is proposed. By incorporating second-order optimization and a trap-avoidance mechanism, the NRBO-BP algorithm effectively adjusts weight update directions, suppresses ineffective training iterations, and enhances global search capability. Simulation results demonstrate that the proposed method significantly improves both prediction accuracy and training performance. The NRBO-BP algorithm provides a reliable and efficient solution for real-time FSO link quality assessment, offering strong support for adaptive performance optimization and stable system operation in complex dynamic environments.

Key words: Free space optical communication; Complex dynamic environment; Quality factor; Newton Raphson based optimizer; Backpropagation neural network

OCIS Codes: 060.2605; 010.1330; 010.1310

CSTR: 32255.14.gzxb20265507.0706001

Foundation item: National Natural Science Foundation of China (61471130); Guangdong Provincial Key Area R&D Program Fund (2019B010138004).